

Non-negligible factors in low-pressure sprinkler irrigation: droplet impact angle and shear stress

HUI Xin¹, ZHENG Yudong¹, MUHAMMAD Rizwan Shoukat¹, TAN Haibin³, YAN Haijun^{1,2*}

¹ College of Water Resources and Civil Engineering, China Agricultural University, Beijing 100083, China;

² Engineering Research Center of Agricultural Water-Saving and Water Resources, Ministry of Education, Beijing 100083, China;

³ Semi-arid Agriculture Engineering & Technology Research Center of China, Shijiazhuang 050051, China

Abstract: Droplet shear stress is considered as an important indicator that reflects soil erosion in sprinkler irrigation more accurately than kinetic energy, and the effect of droplet impact angle on the shear stress cannot be ignored. In this study, radial distribution of droplet impact angles, velocities, and shear stresses were investigated using a two-dimensional video disdrometer with three types of low-pressure sprinkler (Nelson D3000, R3000, and Komet KPT) under two operating pressures (103 and 138 kPa) and three nozzle diameters (3.97, 5.95, and 7.94 mm). Furthermore, the relationships among these characteristical parameters of droplet were analyzed, and their influencing factors were comprehensively evaluated. For various types of sprinkler, operating pressures, and nozzle diameters, the smaller impact angles and larger velocities of droplets were found to occur closer to the sprinkler, resulting in relatively low droplet shear stresses. The increase in distance from the sprinkler caused the droplet impact angle to decrease and velocity to increase, which contributed to a significant increase in the shear stress that reached the peak value at the end of the jet. Therefore, the end of the jet was the most prone to soil erosion in the radial direction, and the soil erosion in sprinkler irrigation could not only be attributed to the droplet kinetic energy, but also needed to be combined with the analysis of its shear stress. Through comparing the radial distributions of average droplet shear stresses among the three types of sprinklers, D3000 exhibited the largest value (26.94–3313.51 N/m²), followed by R3000 (33.34–2650.80 N/m²), and KPT (16.15–2485.69 N/m²). From the perspective of minimizing the risk of soil erosion, KPT sprinkler was more suitable for low-pressure sprinkler irrigation than D3000 and R3000 sprinklers. In addition to selecting the appropriate sprinkler type to reduce the droplet shear stress, a suitable sprinkler spacing could also provide acceptable results, because the distance from the sprinkler exhibited a highly significant ($P<0.01$) effect on the shear stress. This study results provide a new reference for the design of low-pressure sprinkler irrigation system.

Keywords: center pivot irrigation system; water droplet; universal model; soil erosion; water-saving irrigation

Citation: HUI Xin, ZHENG Yudong, MUHAMMAD Rizwan Shoukat, TAN Haibin, YAN Haijun. 2022. Non-negligible factors in low-pressure sprinkler irrigation: droplet impact angle and shear stress. Journal of Arid Land, 14(11): 1293–1316. <https://doi.org/10.1007/s40333-017-0029-5>

1 Introduction

The lack of rainfall in arid and semi-arid areas inevitably makes sprinkler irrigation as one of the significant alternatives and an important way to supplement water to crops in these areas (Stambouli et al., 2013; Etikala et al., 2021). However, soil surface sealing or crusting occurs

*Corresponding author: YAN Haijun (E-mail: yanlj@cau.edu.cn)

Received 2022-05-13; revised 2022-09-26; accepted 2022-10-19

© Xinjiang Institute of Ecology and Geography, Chinese Academy of Sciences, Science Press and Springer-Verlag GmbH Germany, part of Springer Nature 2022

often during sprinkler irrigation. This not only alleviates the infiltration rate of soil, but also leads to the surface runoff, resulting in the loss of soil, water, and fertilizer in the farmland (Silva, 2006; de Jong et al., 2011). Previous studies have shown that soil surface sealing was primarily caused by the detachment of soil particles (Lu et al., 2016; Vaezi et al., 2017), and commonly attributed to the droplet kinetic energy (Yan et al., 2011; King and Bjorneberg, 2012a; Al-Kayssi and Mustafa, 2016). Nevertheless, some researchers have observed that mechanistically, the detachment of soil particles from aggregates was closely related to the shear stress generated by the impact of a droplet on the ground, but not to the droplet kinetic energy (Huang et al., 1982; Chang and Hills, 1993a; Ghadiri and Payne, 2010). Therefore, further systematic explorations of droplet shear stress are still required and highly demanded for the effective development of sprinkler irrigation systems.

To date, several studies have focused on the distribution of droplet shear stresses and the impact of droplets on the ground. For example, Huang et al. (1982) used a marker and cell numerical technique to simulate the impact of raindrops on a rigid surface, and found that the distribution of impact pressure was non-uniform, i.e., the maximum pressure occurred at the contact circumference, and the rebound velocity on the rigid surface was twice the impact velocity. Ferreira et al. (1985) used the principle of energy balance and a modified solution algorithm-volume of fluid (SOLA-VOF) numerical simulation scheme for investigating the impact of raindrops in a deep pool. They found that the fragmentation of most soil aggregates appeared in the formation of crater due to the impact pressure and shear stress on the bottom of the pool. Moreover, Ghadiri and Payne (1986) used the water-hammer theory to evaluate the compressive stress of falling raindrop and shear stress caused by flow impact. They found that the shear stress was several times higher than the compressive stress. It was obvious that the droplets involved in the above-mentioned studies were mainly the raindrops. However, in general, the raindrops impact the ground vertically, which is fundamentally different from the droplets impacting the ground at oblique angles in sprinkler irrigation. Consequently, for determining the distribution characteristics of shear stresses when sprinkler droplets impact the ground, Chang and Hills (1993b) employed the full three-dimensional (3D) Navier-Stokes equations and finite difference procedure to propose a numerical model and used this model to simulate the pressure and shear stress distributions of sprinkler droplets on the surface of soil. Results indicated that, compared with the vertical droplet impact, the oblique droplet impact decreased the magnitude of impact force, and increased the shear stress. Again, Chang and Hills (1993a) conducted laboratory experiments to study the effect of droplet impact angles on the soil infiltration under sprinkler irrigation, and found that the average steady infiltration rates for all soil types gradually increased in the order of impact angles of 60°, 45°, and 90°. These findings indicated that the impact angle of sprinkler droplet significantly influenced the distribution of shear stress and soil infiltration. However, only three droplet impact angles were considered in their research, which was not sufficient to reflect the multi-angle impact of droplets on the ground in actual sprinkler irrigation. Based on this result, Hui et al. (2021a) considered a ball-driven sprinkler as the research object and used a two-dimensional video disdrometer (2DVD) to investigate the radial distributions of droplet impact angles corresponding to three operating pressures and two nozzle diameters. Furthermore, the relationships between droplet impact angles and shear stresses under different working conditions were established. The study provided a new method for accurately predicting the soil erosion under sprinkler irrigation. However, the structure of ball-driven sprinkler was relatively unique, due to which, the conclusions drawn from the study might not provide the guiding significance for farmland irrigation.

As one of the common high-efficiency water-saving irrigation devices in farmland, the center pivot irrigation system has rapidly applied in China in recent years due to its advantages including high irrigation efficiency, wide coverage of irrigated area, high automation, and low labor costs (Yan et al., 2020; Baiamonte et al., 2021; Hui et al., 2022a). By the end of 2019, there were more than 18×10^3 sets of center pivot and linear-move irrigation systems used in China, with an

irrigation area of nearly $6 \times 10^5 \text{ hm}^2$, which accounted for about 14.2% of the total sprinkler irrigation area (Hui et al., 2022b). With the global objective of peaking the carbon emissions and carbon neutrality, it is imperative to realize the low-pressure and energy-saving sprinkler irrigation. According to previous studies, low-pressure sprinkler irrigation could not only significantly reduce energy consumption, but also ensure yield and water use efficiency (Robles et al., 2017). Recently, the use of center pivot has led to gradual replacement of medium- and high-pressure sprinklers with low-pressure sprinklers to minimize the energy requirement of the system. The low-pressure sprinklers are commonly classified into three types, namely the fixed spray plate sprinkler (FSPS), rotating spray plate sprinkler (RSPS), and oscillating spray plate sprinkler (OSPS) (Manke et al., 2019; Hui et al., 2021b). The different structures and operating modes of these three types of sprinkler result in significant differences in their performances. Among them, the cost of FSPS is lower than that of RSPS. However, this type of sprinkler attains high instantaneous application rates and poor application uniformity (Silva, 2007; Yan et al., 2011). In contrast, RSPS has higher energy consumption, despite its wide spraying range and relatively uniform water distribution (Faci et al., 2001; Chen et al., 2020; Hui et al., 2022a). Nonetheless, the strong wind resistance characteristics of OSPS make it highly competitive in the sprinkler marketplace (Manke et al., 2019). Nowadays, numerous studies have focused on the water application rate, droplet diameter, kinetic energy, and other indicators of low-pressure sprinklers (Yan et al., 2010; Sayyadi et al., 2014; Robles et al., 2019; Hui et al., 2022b). However, the impact angle and shear stress of the droplet have rarely been investigated, which is not conducive to further revealing the soil erosion mechanism under low-pressure sprinkler irrigation.

The main objectives of this study are (1) to investigate the radial distribution of droplet impact angles under the three types of low-pressure sprinkler with two operating pressures and three nozzle diameters; (2) to evaluate the relationships among the distance from sprinkler, droplet impact angle, and shear stress, as well as the relationships among droplet impact angle, velocity, and shear stress; (3) to establish the mathematical models among the above mentioned indicators; and (4) to further determine the effects of various factors on droplet impact angle, velocity, and shear stress.

2 Materials and methods

2.1 Experimental setup

A droplet distribution test of a single sprinkler was conducted to comprehensively investigate the droplet impact angles and shear stresses of low-pressure sprinklers of the center pivot irrigation system. The tested three types of sprinkler were the Nelson D3000 (Nelson Irrigation Corp., Walla Walla, USA) with a fixed spray plate sprinkler equipped with a 36-grooved blue plate, the Nelson R3000 with a rotating spray plate sprinkler equipped with a 10-grooved brown plate, and the Komet KPT (Komet Irrigation Corp., Lienz, Austria) with an oscillating spray plate sprinkler and a 10-grooved black plate, as shown in Figure 1. In each test, the sprinkler could be matched with a corresponding pressure regulator to obtain the required stable operating pressure. Moreover, the three types of sprinkler used in this study were all installed upside down. Therefore, the upper part of the pressure regulator was closely connected with the elbow of the height-adjustable riser. The riser was cast from steel, which exhibited high strength and no shaking during sprinkler irrigation. Furthermore, a manual valve and a pressure gauge with the accuracy of 0.4% (MIK-Y190, Asmik Sensors Technology Co., Ltd., Hangzhou, China) were installed on the riser for real-time monitoring and adjustment of operating pressure. Water required for sprinkler irrigation was obtained from a stainless-steel water tank and pressurized before sent to the inlet of the sprinkler using centrifugal pump (IS80-50-250, Foshan Pump Factory Co., Ltd., Foshan, China). Meanwhile, an electromagnetic flowmeter with the accuracy of 0.5% (E-mag E, Kaifeng Instrument Co., Ltd., Kaifeng, China) was used to measure the flow rate in the pipeline.

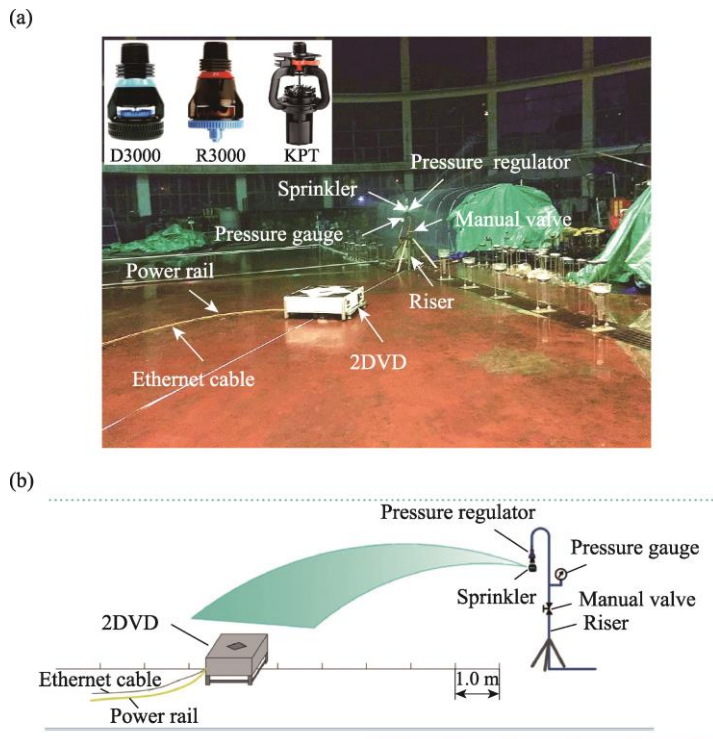


Fig. 1 Test for the droplet of low-pressure sprinkler. (a), scenario of test; (b), schematic of test.

It was noted that the acquisition of droplet characteristical parameters was achieved by the 2DVD (Joanneum Research Corp., Graz, Austria), which is regarded as the most advanced equipment for the measurement of precipitation particle at the global scale. This equipment mainly consists of a measurement device, a laptop, and a power supply unit (Fig. 2a), which can monitor the size, shape, aggregation state, falling velocity, and the direction of a single precipitation event (such as rain, snow, and hail). Moreover, 2DVD has been used in many fields, such as meteorology and environment, telecommunications and wave propagation, and other industrial applications (Kruger and Krajewski, 2002; Huang et al., 2010). During the sprinkler droplet test, the two perpendicularly disposed charge coupled device cameras (cameras A and B) inside the 2DVD instrument could scan the droplets passing through the measurement area ($100 \text{ mm} \times 100 \text{ mm}$; Fig. 2b), and record the vertical and horizontal velocity components of each droplet (Ge et al., 2020). The test accuracy of the droplet diameter of 2DVD could reach 0.19 mm . In addition to the above-mentioned devices, the tape measure (DL9830, Deli group, Ningbo, China), stopwatch (PC2810, Shenzhen Timestar Electronic Co., Ltd., Shenzhen, China), as well as the wet and dry bulb thermometers (DL9013, Deli group, Ningbo, China) were also used in the test.

2.2 Experimental design

An indoor experiment for sprinkler irrigation was conducted at the Research Center of Fluid Machinery Engineering and Technology, Jiangsu University, Zhenjiang, China. The experiment was carried out under no wind conditions with an air temperature of 10°C and relative humidity of 60%. In the design of droplet distribution test, various factors such as sprinkler type (D3000, R3000, and KPT), nozzle diameter (3.97 mm, 5.95 mm, and 7.94 mm), and operating pressure (103 and 138 kPa) were considered. A total of 18 trials were conducted. The specific working parameters and the corresponding flow rates of sprinklers are listed in Table 1. More importantly, due to the different manufacturers of KPT, D3000, and R3000, a certain difference in flow rate between KPT and other two types of sprinkler was observed. However, their maximum difference under the same nozzle diameter and operating pressure did not exceed $0.07 \text{ m}^3/\text{h}$, indicating that the accuracy of the test could still be guaranteed.

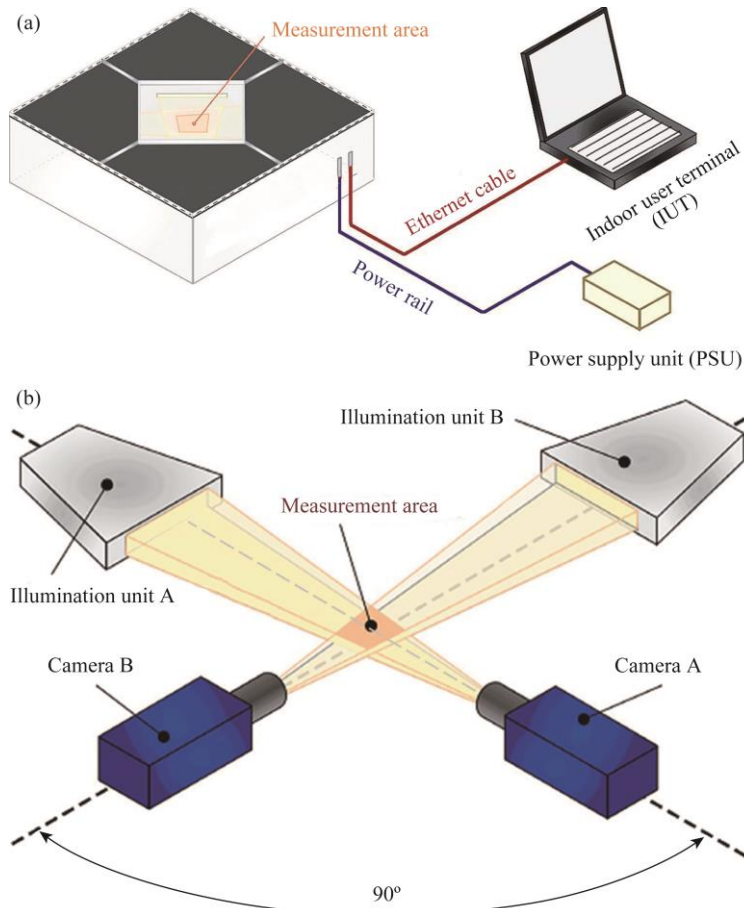


Fig. 2 2DVD instrument for measuring droplets. (a), composition of 2DVD; (b), schematic of measuring planes of 2DVD.

Table 1 Working parameters and corresponding flow rates of the three types of low-pressure sprinkler

Sprinkler type	Operating pressure (kPa)	Nozzle diameter (mm)	Flow rate (m^3/h)
D3000	103	3.97	0.61
		5.95	1.38
		7.94	2.46
	138	3.97	0.70
		5.95	1.59
		7.94	2.84
R3000	103	3.97	0.61
		5.95	1.38
		7.94	2.46
	138	3.97	0.70
		5.95	1.59
		7.94	2.84
KPT	103	3.97	0.64
		5.95	1.43
		7.94	2.47
	138	3.97	0.74
		5.95	1.66
		7.94	2.86

The distribution of droplets was analyzed using individual sprinkler irrigation. Before the test, we adjusted the sprinkler to a height of 1.2 m above the cameras of 2DVD instrument to maintain similarity to the sprinkler mounting height used in the center pivot irrigation systems (Hui et al., 2022a). Then, the water supply system was turned on, and 2DVD was used to collect the information regarding the droplet velocity under certain stabilized pressure and flow rate conditions. The measuring points of water droplets were arranged at the intervals of 1 m in the radial direction within the radius of throw, and the number of effective droplets obtained at each measuring point was kept at about one thousand (Fig. 1). After the droplet data of all measuring points were collected, the 3σ criterion (Pauta criterion that is one of the criteria for checking erroneous data) was used to check and eliminate the error in data caused by droplet splashing (Jiang et al., 2021).

2.3 Calculations

The resultant velocity of droplet (hereinafter referred to as droplet velocity) is calculated using the vertical and horizontal velocities of the water droplet recorded using 2DVD, and expressed as Equation 1.

$$V = \sqrt{V_v^2 + V_h^2}, \quad (1)$$

where V is the resultant velocity of the droplet (m/s); V_v is the vertical velocity of the droplet (m/s); and V_h is the horizontal velocity of the droplet (m/s).

The impact angle of droplet represents the angle between the direction of droplet impacting the ground and the soil surface, and is calculated by Equation 2.

$$\theta = \frac{180}{\pi} \arctan\left(\frac{V_v}{V_h}\right), \quad (2)$$

where θ is the impact angle of the droplet ($^\circ$).

Equation 3 is used for calculating the shear stress of droplet (horizontal stress generated by the droplet impacting the ground) (Ghadiri and Payne, 1986).

$$S_s = 0.5\rho V_h^2, \quad (3)$$

where S_s is the shear stress of droplet (N/m²); and ρ is the mass density of droplet (kg/m³).

2.4 Data analysis

Regression analysis was performed using the Origin 8.5 software (OriginLab, Northampton, MA, USA), and Matlab R2010a software (MathWorks, Natick, MA, USA) was applied to develop the relationships among droplet impact angle, distance from sprinkler, droplet velocity, and shear stress as well as the relationship between droplet shear stress and distance from sprinkler. Coefficient of determination (R^2) was used to assess the fitting accuracies of these relationships, whereas mean absolute error (MAE) and root mean square error (RMSE) between simulated and measured values were used to verify the accuracy of relationship. Meanwhile, coefficient of variation (CV) was used to evaluate the degree of dispersion of droplet impact angles under different distances from sprinkler. The higher the CV, the more discrete the distribution of droplet impact angles. Moreover, the effects of sprinkler type, operating pressure, nozzle diameter, and distance from sprinkler on the droplet impact angle, velocity, and shear stress were subjected to multivariate analysis of variance (MANOVA). Mean values were separated using the Fisher's protected least significant difference (LSD) at 0.05 level by using SPSS 20.0 software (IBM Corp., Armonk, NY, USA).

3 Results

3.1 Radial distribution of droplet impact angles

Figures 3 and 4 showed the radial distributions of droplet impact angles for the three types of sprinkler with three nozzle diameters and two operating pressures. It could be observed that

irrespective of working conditions employed, the relative frequencies of droplet impact angles within the range of 70°–90° averaged 95.8% within 3 m distance from sprinkler. With the increase in the distance from sprinkler, the number of droplets with the impact angles of 70°–90° gradually decreased, and the droplets with the impact angle of less than 70° increased correspondingly. When the distance from sprinkler reached 5 m, the average relative frequency of droplets with the impact angles of 70°–90° varied under different treatments, attaining the average of only 49.9%, which was 46.2% lower than that of the droplets with 3 m distance. Therefore, Figures 3 and 4 clearly demonstrated that these reduced 70°–90° droplets shifted to the range of 60°–70°, making the average relative frequency of droplets in this impact angle range reach 48.5% under different treatments. In summary, changing the distance from sprinkler could effectively alter the distribution of droplet impact angles. In other words, the throw radius of low-pressure sprinkler potentially affected the droplet impact angle.

With the continuous increase in the distance from sprinkler, the distribution range of droplet impact angles spreaded further. When the distance was increased to the end of the jet, the relative frequency of droplet impact angles within the range of 50°–60° increased dramatically, while those within the ranges of 60°–70° and even 70°–90° decreased accordingly. The average relative frequencies of these three ranges of droplet impact angles (50°–60°, 60°–70°, and 70°–90°) at the end of the jet were 23.7%, 53.2%, and 23.1%, respectively. From the perspective of overall distribution of droplet impact angles, the number of droplets with medium impact angles (60°–70°) still dominated, although the number of droplets with small impact angles (50°–60°) increased. Consequently, the distribution of relative frequency of droplet impact angles at the end of the jet took the form of a logarithmic distribution. Furthermore, Table 2 showed the radial CVs of

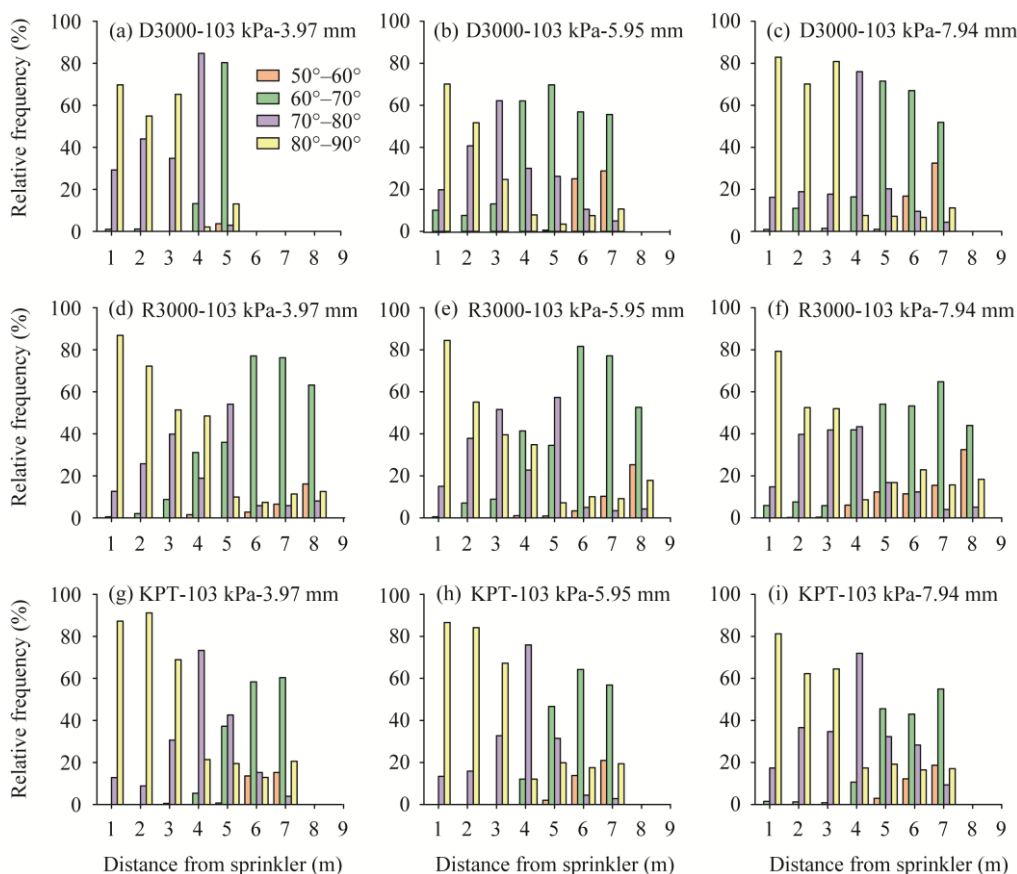


Fig. 3 Relative frequency distributions of droplet impact angles along the spray direction for the three types of sprinkler and three nozzle diameters at an operating pressure of 103 kPa. (a–c), D3000; (d–f), R3000; (g–i), KPT.

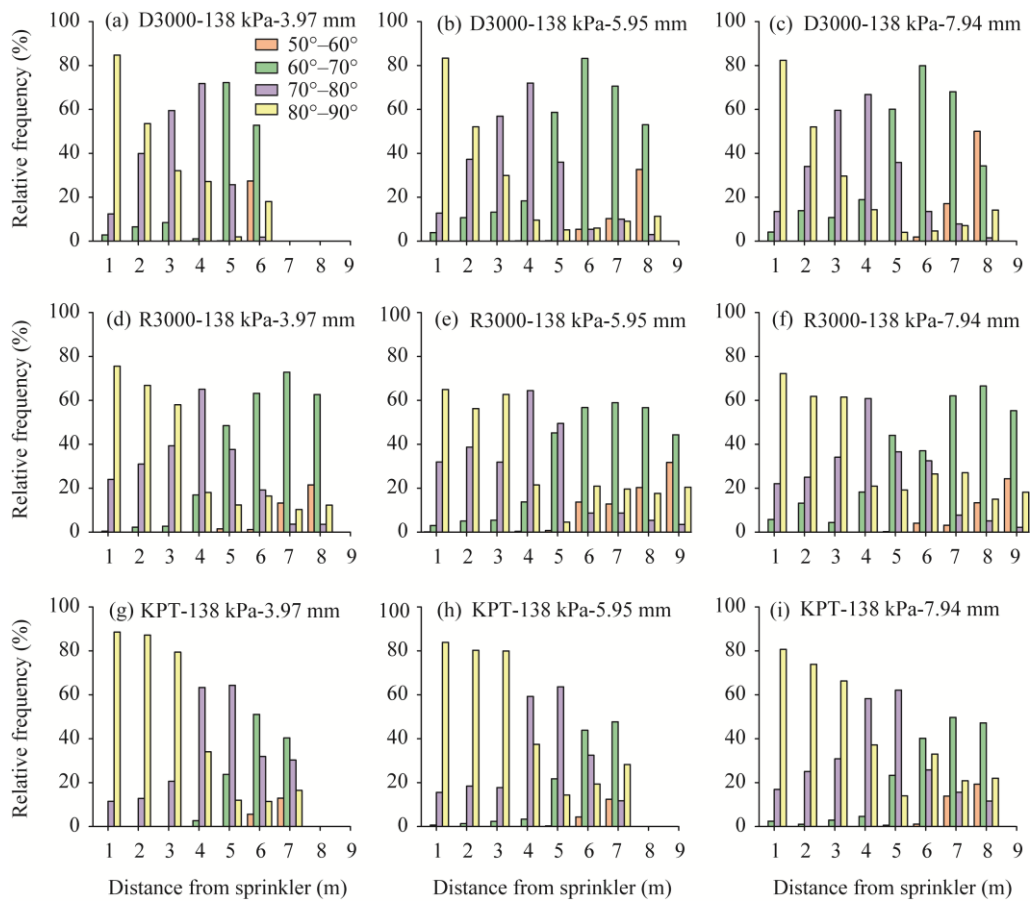


Fig. 4 Relative frequency distributions of droplet impact angles along the spray direction for the three types of sprinkler and three nozzle diameters at an operating pressure of 138 kPa. (a–c), D3000; (d–f), R3000; (g–i), KPT.

Table 2 Coefficients of variation of droplet impact angles along the spray direction under the three types of sprinkler, three nozzle diameters, and two operating pressures

Sprinkler type	Operating pressure (kPa)	Nozzle diameter (mm)	Coefficient of variation (%)								
			1 m	2 m	3 m	4 m	5 m	6 m	7 m	8 m	9 m
D3000	103	3.97	4.70	8.40	9.01	11.91	23.54	-	-	-	-
		5.95	9.37	9.78	10.58	18.53	19.21	20.13	23.44	-	-
		7.94	6.46	7.03	10.03	17.46	18.74	26.59	30.55	-	-
	138	3.97	6.24	8.88	9.17	9.56	19.38	28.17	-	-	-
		5.95	9.33	9.72	10.33	11.64	15.64	18.25	23.97	25.71	-
		7.94	8.86	10.21	10.39	11.31	17.94	18.09	21.68	31.19	-
	R3000	3.97	6.34	7.73	9.69	10.15	13.67	16.02	16.05	17.49	-
		5.95	6.15	8.15	10.96	11.53	12.82	15.72	19.90	20.68	-
		7.94	8.38	10.94	11.61	11.89	18.28	24.42	28.24	28.74	-
KPT	103	3.97	6.71	7.36	7.53	10.18	12.16	13.42	18.10	18.35	-
		5.95	6.92	7.88	8.20	11.12	11.89	17.56	22.92	24.03	24.12
		7.94	8.68	8.73	11.16	12.06	14.28	15.78	16.32	18.08	19.33
	138	3.97	2.74	3.6	3.67	14.56	17.96	19.92	21.59	-	-
		5.95	5.67	5.93	7.40	15.45	21.89	23.47	24.08	-	-
		7.94	6.68	7.26	7.94	13.75	18.32	20.68	23.16	-	-

Note: - represents no data.

droplet impact angles with three types of low-pressure sprinkler. Notably, the higher the distance from the sprinkler, the more discrete the distribution of droplet impact angle. Considering D3000-138 kPa-7.94 mm (sprinkler type-operating pressure-nozzle diameter) as an example, its CVs at 2, 5, and 8 m from sprinkler were 10.21%, 17.94%, and 31.19%, respectively. Therefore, the end of the jet might be the most vigorous area for droplets to break up and collide with each other, thus leading to a very dispersed distribution of droplet impact angle.

3.2 Relationship between droplet impact angle and distance from sprinkler

In order to clarify the relationship between droplet impact angle and distance from sprinkler, radial distribution of average droplet impact angles under the three types of sprinkler with three nozzle diameters and two operating pressures was systematically analyzed, as shown in Figure 5. Overall, the increase in distance from sprinkler caused the average droplet impact angle to decrease, which reached the minimum at the end of the jet. The average droplet impact angles of D3000, R3000, and KPT sprinklers along the spray direction were observed to be distributed within the ranges of 62.12° – 87.26° , 60.08° – 86.30° , and 61.61° – 87.60° , respectively, for three nozzle diameters and two operating pressures.

Figure 5 showed similar radial distributions of average droplet impact angles for three nozzle diameters or two operating pressures with the same type of sprinkler. For instance, at the same distance from sprinkler, the maximum differences of average droplet impact angles among three nozzle diameters and two operating pressures for D3000 remained at around 2.23° and 3.27° , respectively. However, these values changed to 2.84° and 3.51° for R3000, and to 2.72° and 4.11° for KPT. As a result, irrespective of the type of low-pressure sprinkler, the maximum differences of average droplet impact angles under different irrigation treatments existed within the range of 2° – 5° , which was only 2.66%–6.66% of average droplet impact angle (75.06°) for the three types of sprinkler. Taken together, nozzle diameter and operating pressure had little effect on the distribution of droplet impact angle and could be ignored in the design of irrigation system.

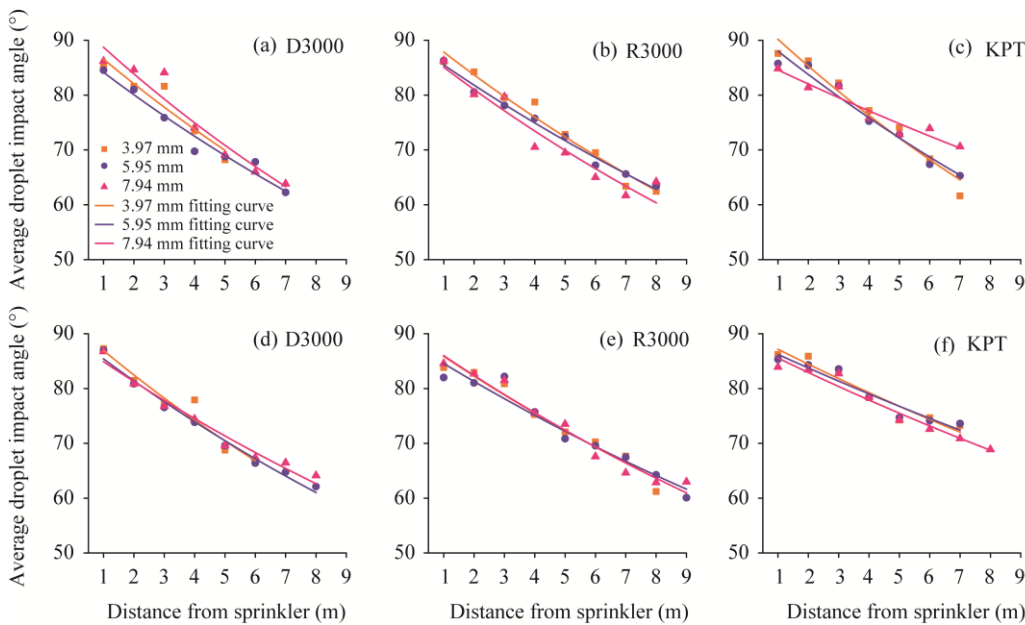


Fig. 5 Average droplet impact angles along the spray direction under the three types of sprinkler, three nozzle diameters, and two operating pressures. (a–c), 103 kPa; (d–f), 138 kPa.

Furthermore, a certain exponential relationship was observed between average droplet impact angle and distance from sprinkler through regression analysis. The specific exponential equations under the three types of sprinkler, three nozzle diameters, and two operating pressures could be expressed by $\bar{\theta} = \alpha e^{\beta l}$, as depicted in Table 3. Apparently, R^2 values of different treatments

exceeded 0.900 except for D3000-103 kPa-3.97 mm treatment that exhibited a slightly lower R^2 (0.866) value. High R^2 values suggested that exponential relationships of these correlations reached an excellent level. Based on these results, it could be inferred that exponential relationship between average droplet impact angle and distance from sprinkler was universal for low-pressure sprinklers used in the center pivot irrigation system. This was also confirmed by the results that droplet impact angle exhibited a weak correlation with its operating pressure and nozzle diameter. The following universal correlation (Eq. 4) was derived by reintegrating the data regarding the average droplet impact angles and distances from sprinkler under different treatments. Comparative analysis between simulated average impact angles and measured values found that the accuracy of correlation was excellent, with MAE and RMSE values of 2.061° and 2.587° , respectively (Fig. 6).

Table 3 Regression equations between average droplet impact angle and distance from sprinkler under the three types of sprinkler, three nozzle diameters, and two operating pressures

Sprinkler type	Operating pressure (kPa)	Nozzle diameter (mm)	Fitting coefficient		R^2
			α	β	
D3000	103	3.97	91.308	-0.053	0.866
		5.95	88.431	-0.050	0.957
		7.94	93.852	-0.056	0.922
	138	3.97	91.614	-0.053	0.923
		5.95	89.594	-0.048	0.984
		7.94	88.654	-0.043	0.967
R3000	103	3.97	92.199	-0.048	0.965
		5.95	89.344	-0.044	0.985
		7.94	89.361	-0.049	0.920
	138	3.97	89.615	-0.043	0.955
		5.95	87.980	-0.040	0.938
		7.94	89.780	-0.043	0.960
KPT	103	3.97	95.355	-0.056	0.949
		5.95	92.484	-0.050	0.959
		7.94	87.231	-0.031	0.915
	138	3.97	89.979	-0.032	0.913
		5.95	88.765	-0.029	0.909
		7.94	88.273	-0.031	0.952

Note: α and β are the fitting coefficients of the equation $\bar{\theta} = \alpha e^{\beta L}$.

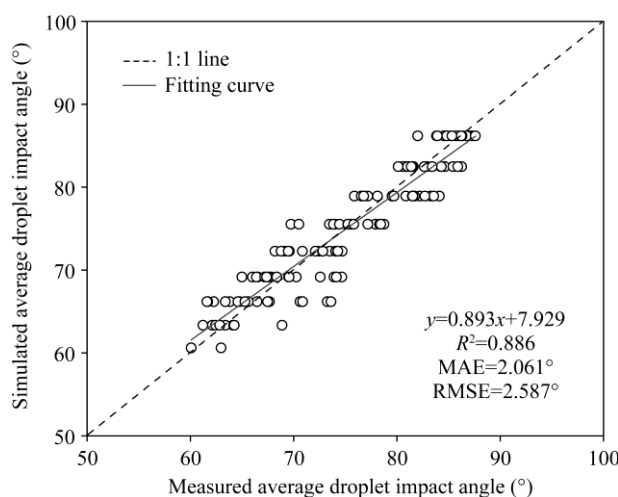


Fig. 6 Comparison between simulated and measured average droplet impact angles obtained by using Equation 4

$$\bar{\theta} = 90.066e^{-0.044l}, R^2 = 0.882, \quad (4)$$

where $\bar{\theta}$ is the average droplet impact angle ($^\circ$); and l is the distance from sprinkler (m).

3.3 Relationship between droplet impact angle and velocity

Figures 7 and 8 illustrated the relationships between radial droplet impact angles and velocities for the three types of sprinkler with three nozzle diameters and two operating pressures. Overall, droplet impact angle initially increased, and then decreased with the increase in velocity. In addition to the strong correlation between droplet velocity and impact angle, distance from sprinkler was also highly correlated to droplet velocity and its impact angle. At the distance of 1 m from sprinkler, droplet velocity distribution ranges of three low-pressure sprinklers (D3000, R3000, and KPT) were distributed within the ranges of 0.56–4.74, 0.62–5.91, and 0.62–5.39 m/s, respectively. Correspondingly, the ranges of droplet impact angles were maintained at 60.75°–90.00°, 53.53°–90.00°, and 65.38°–90.00°, respectively (as shown in Table 4). Among the three types of sprinkler, R3000 had the widest distribution range near sprinkler in terms of both droplet velocity and impact angle. By increasing distance from sprinkler, distribution range of droplet velocities expanded slightly, while that of impact angles shrank. When the distance was increased to 3 m, the maximum droplet velocities and the minimum impact angles of D3000, R3000, and KPT were higher 0.33, 0.56, and 0.32 m/s, and 2.82°, 6.20°, and 2.82°, respectively than those at 1 m. Therefore, within the distance of 3 m from sprinkler, a positive correlation was observed among distance from sprinkler, droplet velocity, and impact angle. The longer the distance from sprinkler, the greater the droplet velocity and impact angle. On the other hand, it demonstrated that, with the increase in velocity, droplet impact angle of R3000 increased faster than those of D3000 and KPT.

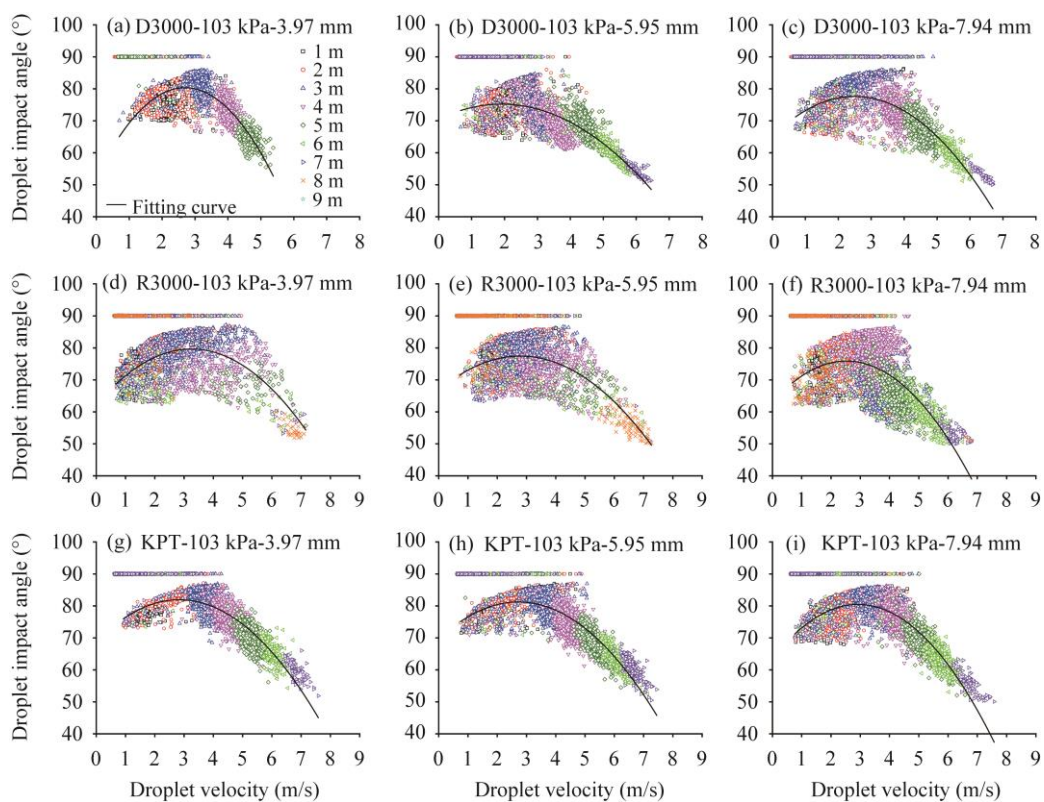


Fig. 7 Relationships between droplet velocities and impact angles along the spray direction for the three types of sprinkler and three nozzle diameters at an operating pressure of 103 kPa. (a–c), D3000; (d–f), R3000; (g–i), KPT.

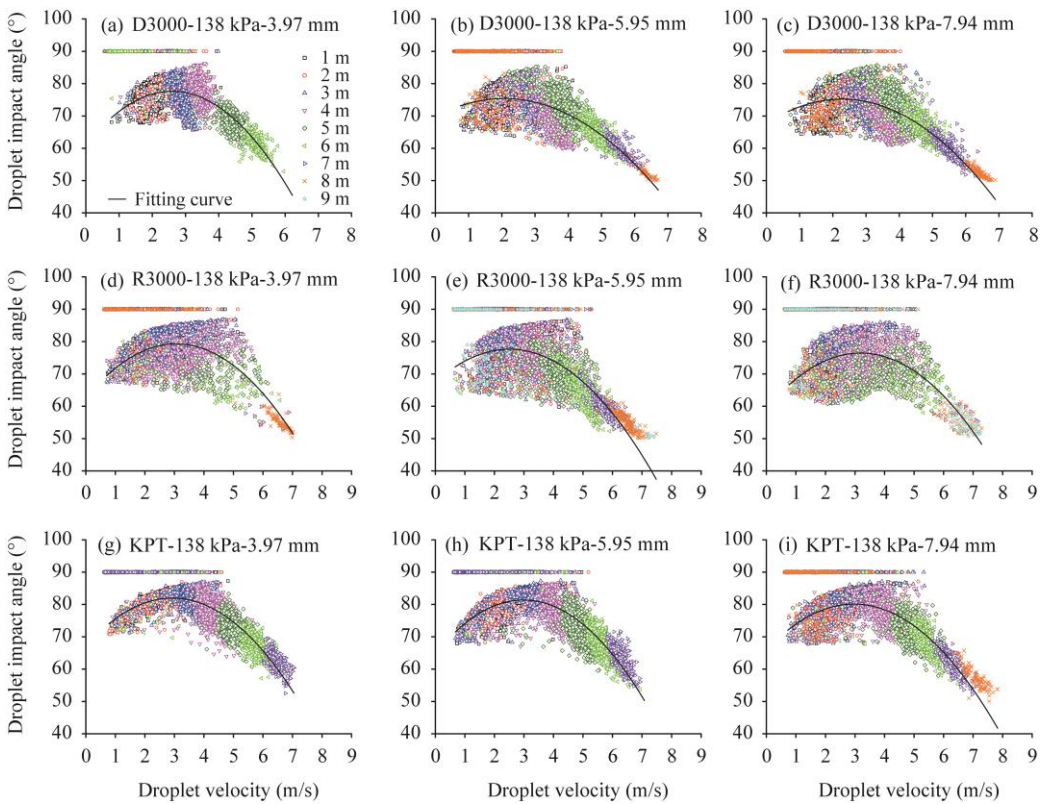


Fig. 8 Relationships between droplet velocities and impact angles along the spray direction for the three types of sprinkler and three nozzle diameters at an operating pressure of 138 kPa. (a–c), D3000; (d–f), R3000; (g–i), KPT.

With the increase in distance from sprinkler, distribution range of droplet velocities and impact angles of each sprinkler began to expand rapidly. When the distance from sprinkler was 5 m, the maximum droplet velocities of the three types of sprinkler increased by 1.27 m/s on average compared with those at the distance of 3 m. In particular, the average reduction of their minimum impact angles reached 10.80°, a decrease of more than 16%. With the increase in velocity, the variation trend of droplet impact angle changed from a gradual increase to a continuous fall at 3–5 m away from sprinkler. When the distance exceeded 5 m, any further increase in distance from sprinkler could still bring a continuous increase in droplet velocity and successive decrease in impact angle. However, the results in Table 4 clearly showed that droplet velocity and impact angle distribution ranges of several measuring points (6, 7, and 8 m) near the end of the jet were very close to each other, indicating the stabilization of variation trends. Finally, droplet velocities of D3000, R3000, and KPT at 8 m were stable within the ranges of 0.62–7.00, 0.62–8.76, and 0.62–7.46 m/s, respectively, whereas the corresponding ranges for droplet impact angles were 50.03°–90.00°, 50.19°–90.00°, and 50.03°–90.00°, respectively. Overall, the end of the jet produced the highest droplet velocity and the smallest impact angle, which resulted in the highest shear stress during the entire trajectory of jet.

Furthermore, regression analysis for the relationships between radial droplet velocities and impact angles under different types of sprinkler, nozzle diameters, and operating pressures was conducted (Figs. 7 and 8). It was found that the relationship between droplet velocity and impact angle could be expressed as: $\theta = \gamma V^2 + \delta V + \varepsilon$, in which γ , δ , and ε are the fitting coefficients. Table 5 showed the result of regression analysis. Noticeably, R3000 sprinkler showed the worst fitting accuracy, and its average R^2 value was only 0.407 under different working conditions. One possible explanation was that R3000 showed an irregular plate structure, which affected the

Table 4 Droplet velocity and impact angle range at different distances from sprinkler for the three types of sprinkler with three nozzle diameters and two operating pressures

Sprinkler type	Distance from sprinkler (m)	Droplet velocity (m/s)		Droplet impact angle (°)	
		Maximum	Minimum	Maximum	Minimum
D3000	1	4.74	0.56	90	60.75
	2	4.77	0.55	90	61.92
	3	5.07	0.57	90	63.57
	4	6.05	0.59	90	59.72
	5	6.20	0.63	90	55.48
	6	6.38	0.62	90	51.21
	7	6.83	0.62	90	50.02
	8	7.00	0.62	90	50.03
R3000	1	5.91	0.62	90	53.53
	2	5.95	0.63	90	57.29
	3	6.47	0.63	90	59.73
	4	7.29	0.62	90	53.92
	5	8.02	0.62	90	51.57
	6	7.85	0.62	90	50.10
	7	8.67	0.62	90	50.04
	8	8.76	0.62	90	50.19
KPT	1	5.39	0.62	90	65.38
	2	5.39	0.63	90	67.77
	3	5.71	0.62	90	68.20
	4	6.12	0.62	90	60.58
	5	6.83	0.62	90	52.05
	6	7.41	0.62	90	51.63
	7	8.33	0.62	90	50.08
	8	7.46	0.62	90	50.03

Table 5 Regression analysis between droplet velocity and impact angle along the spray direction for the three types of sprinkler with three nozzle diameters and two operating pressures

Sprinkler type	Operating pressure (kPa)	Nozzle diameter (mm)	Fitting coefficient			R^2
			γ	δ	ε	
D3000	103	3.97	-3.848	20.741	52.391	0.722
		5.95	-1.289	4.918	70.501	0.614
		7.94	-1.992	9.935	65.232	0.680
	138	3.97	-2.457	12.763	61.068	0.670
		5.95	-1.313	5.430	69.781	0.577
		7.94	-1.458	6.643	67.636	0.624
R3000	103	3.97	-1.656	10.763	62.163	0.314
		5.95	-1.384	7.713	66.693	0.338
		7.94	-2.015	10.180	63.037	0.433
	138	3.97	-1.778	10.877	62.652	0.404
		5.95	-1.625	8.143	67.441	0.599
		7.94	-1.676	10.686	59.410	0.351
KPT	103	3.97	-1.634	9.265	68.780	0.784
		5.95	-1.583	8.607	69.527	0.789
		7.94	-1.985	11.591	63.516	0.720
	138	3.97	-1.730	10.125	67.158	0.785
		5.95	-1.855	11.073	64.842	0.727
		7.94	-1.619	9.590	65.924	0.685

Note: γ , δ , and ε are the fitting coefficients of the equation $\theta = \gamma V^2 + \delta V + \varepsilon$.

distribution of droplet velocities and impact angles. In contrast, fitting accuracies of both D3000 and KPT sprinklers were acceptable, with average R^2 values of 0.648 and 0.748, respectively. The above results signified that appropriate low-pressure sprinkler type played an important role in the distribution of droplets. Similarly, droplet velocity and impact angle data under the three types of sprinkler, three nozzle diameters, and two operating pressures were also integrated. A universal correlation was deduced, as represented by Equation 5. Comparative analysis of simulated and measured values clearly indicated that accuracy of correlation was poor, with MAE and RMSE values as high as 7.876° and 9.627°, respectively (Fig. 9).

$$\theta = -1.462V^2 + 7.699V + 67.518, R^2 = 0.452, \quad (5)$$

Where θ is the droplet impact angle (°); and V is the resultant velocity of the droplet (m/s).

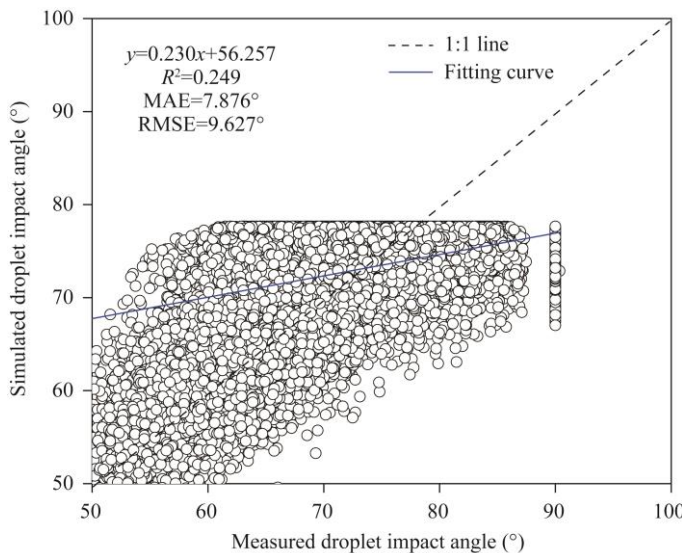


Fig. 9 Comparison between simulated and measured droplet impact angles using Equation 5

3.4 Relationship between droplet impact angle and shear stress

Figures 10 and 11 showed relationship between droplet impact angles and shear stresses for the three types of sprinkler with three nozzle diameters and two operating pressures. Apparently, the larger the droplet impact angle, the smaller the shear stress. This was not surprising because a larger droplet velocity tended to result in a smaller impact angle due to the increased shear stress (Figs. 7 and 8).

Moreover, droplet shear stress was also found to increase gradually with the increase of distance from sprinkler, and reached the maximum value at the end of the jet, as supported by the data presented in Table 6. Considering the distances of 2, 5, and 8 m from sprinkler as an example, droplet shear stresses of D3000 lied within the ranges of 0.00–1740.05, 0.00–4317.32, and 0.00–9720.36 N/m², respectively. Correspondingly, they were within the ranges of 0.00–4082.97, 0.00–6289.79, and 0.00–14,532.66 N/m² for R3000, respectively; within 0.00–1122.19, 0.00–8145.64, and 0.00–11,748.69 N/m² for KPT, respectively. It was not difficult to find that droplet shear stress range for R3000 near the sprinkler (2 m) was much larger than those for other two sprinklers, and its maximum droplet shear stress was 2.35 and 3.64 times those of D3000 and KPT sprinklers, respectively. This was mainly attributed to the fact that the distribution of droplet velocities and impact angles lied within wider ranges for R3000 near the sprinkler than those of other two sprinklers.

However, when distance was increased, distribution ranges of droplet shear stresses for the three types of sprinkler began to expand gradually, among which KPT exhibited the fastest expansion, followed by D3000 and R3000. Therefore, when distance was increased to the middle of the jet (5 m), the maximum droplet shear stresses for the three types of sprinklers increased

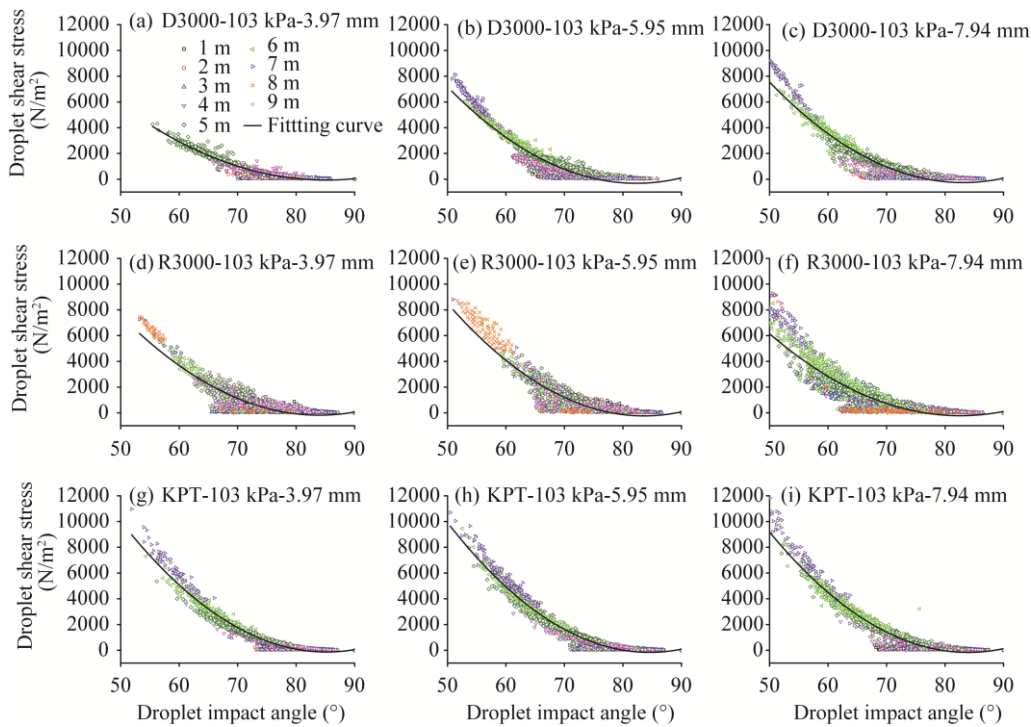


Fig. 10 Relationships between droplet impact angles and shear stresses along the spray direction for the three types of sprinkler and three nozzle diameters at an operating pressure of 103 kPa. (a–c), D3000; (d–f), R3000; (g–i), KPT.

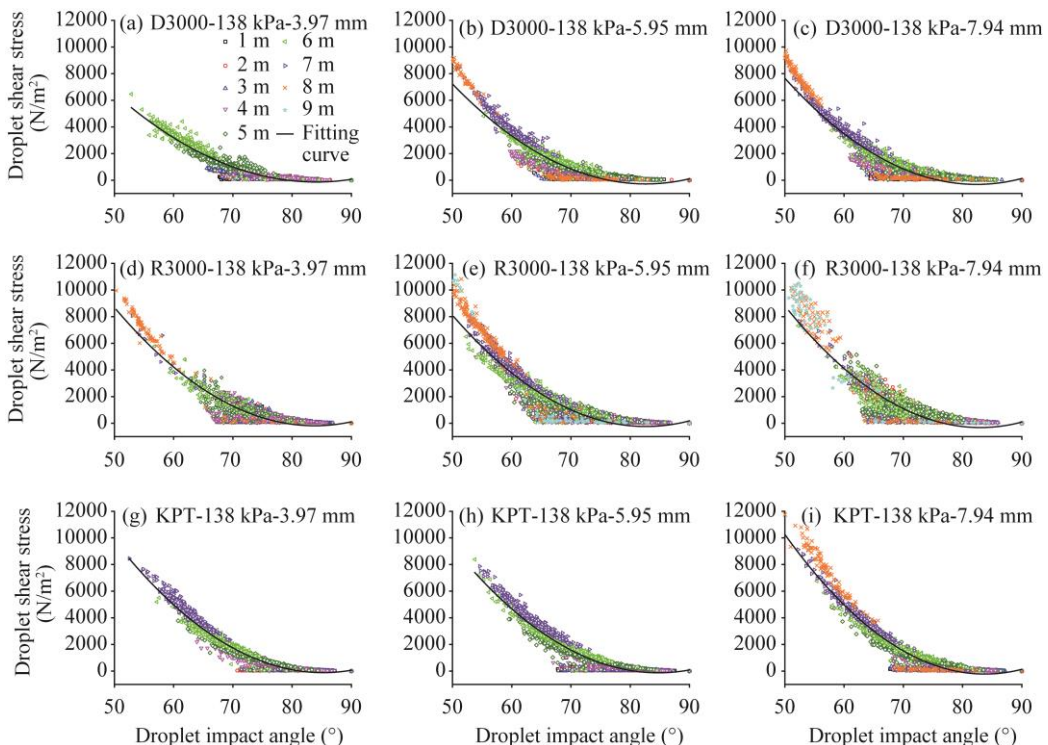


Fig. 11 Relationships between droplet impact angles and shear stresses along the spray direction for the three types of sprinkler and three nozzle diameters at an operating pressure of 138 kPa. (a–c), D3000; (d–f), R3000; (g–i), KPT.

Table 6 Droplet shear stress ranges at different distances from sprinkler for the three types of sprinkler with three nozzle diameters and two operating pressures

Sprinkler type	Distance from sprinkler (m)	Droplet shear stress (N/m ²)	
		Maximum	Minimum
D3000	1	1223.65	0.00
	2	1740.05	0.00
	3	1513.85	0.00
	4	2202.85	0.00
	5	4317.32	0.00
	6	6902.65	0.00
	7	9233.80	0.00
	8	9720.36	0.00
R3000	1	3153.58	0.00
	2	4082.97	0.00
	3	3861.14	0.00
	4	5444.54	0.00
	5	6289.79	0.00
	6	8506.57	0.00
	7	9285.09	0.00
	8	14,532.66	0.00
KPT	1	1101.42	0.00
	2	1122.19	0.00
	3	1866.53	0.00
	4	4313.97	0.00
	5	8145.64	0.00
	6	9681.45	0.00
	7	11,820.66	0.00
	8	11,748.69	0.00

by 7023.45, 2577.27, and 2206.82 N/m², respectively, in which droplet shear stress range of KPT exceeded that of R3000. Nevertheless, this trend did not remain the same with a further increase in the distance from sprinkler. When approaching the end of the jet, R3000 showed a sharp expansion for distribution range of droplet shear stress, while expansion of KPT became increasingly slow. Eventually, droplet shear stress range of R3000 exceeded that of KPT when it reached the end of the jet (8 m). In contrast, droplet shear stress range of D3000 was still smaller than those of other two sprinklers, which was related to the steady expansion of droplet shear stress range along radial direction.

Regression correlations between droplet impact angles and shear stresses for the three types of sprinkler with three nozzle diameters and two different operating pressures were shown in Table 7. Clearly, these regression correlations under different working conditions showed good fitting accuracies (average value of R^2 was 0.906). Equation 6 was a universal correlation derived by integrating the data of droplet impact angles and shear stresses under different treatments of low-pressure sprinklers, and its R^2 value was 0.862. Overall, although R^2 value was reduced compared with those obtained using individual regression correlations, it still showed a high accuracy in predicting droplet shear stress. Figure 12 showed comparative analysis of simulated and measured values. Obviously, correlation accuracy was quite good, and its MAE and RMSE values were 214.542 and 418.134 N/m², respectively.

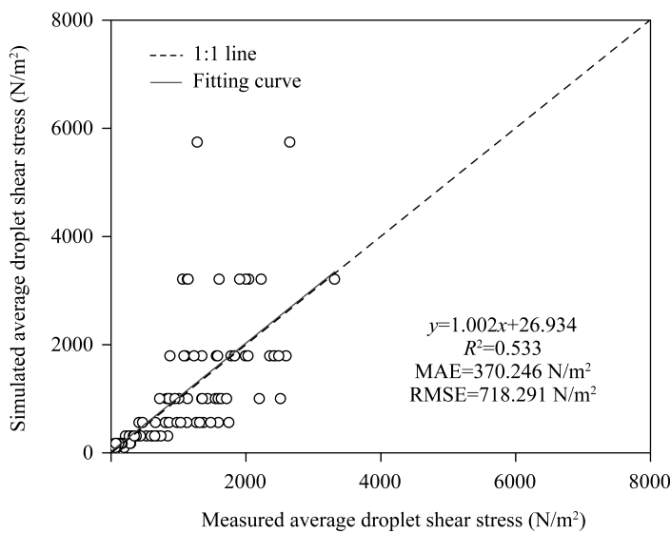
$$S_s = 6.996\theta^2 - 1170.371\theta + 48765.045, R^2 = 0.862, \quad (6)$$

where S_s is the droplet shear stress (N/m²); and θ is the droplet impact angle (°).

Table 7 Regression analysis between droplet impact angle and shear stress along the spray direction for the three types of sprinkler with three nozzle diameters and two operating pressures

Sprinkler type	Operating pressure (kPa)	Nozzle diameter (mm)	Fitting coefficient			R^2
			ζ	η	λ	
D3000	103	3.97	4.744	-807.248	34,272.713	0.933
		5.95	7.182	-1182.318	48,335.269	0.909
		7.94	7.139	-1186.014	48,995.740	0.920
	138	3.97	5.733	-963.945	40,382.961	0.938
		5.95	7.045	-1164.314	47,827.132	0.888
		7.94	7.614	-1254.291	51,337.901	0.912
R3000	103	3.97	6.724	-1128.915	47,204.564	0.838
		5.95	7.735	-1293.528	53,843.836	0.830
		7.94	6.003	-991.281	40,701.654	0.841
	138	3.97	7.772	-1302.684	54,395.948	0.879
		5.95	7.837	-1295.341	53,283.154	0.896
		7.94	8.387	-1392.267	57,456.475	0.853
KPT	103	3.97	8.198	-1397.036	59,382.962	0.961
		5.95	8.454	-1429.439	60,260.384	0.962
		7.94	8.104	-1360.900	56,963.905	0.941
	138	3.97	7.995	-1362.728	57,952.841	0.955
		5.95	7.835	-1328.225	56,164.646	0.926
		7.94	9.194	-1540.344	64,294.587	0.918

Note: ζ , η , and λ are the fitting coefficients of the equation $S_s = \zeta\theta^2 + \eta\theta + \lambda$.

**Fig. 12** Comparison between simulated and measured droplet shear stresses obtained using Equation 6

3.5 Relationship between droplet shear stress and distance from sprinkler

Figure 13 showed radial distribution of average droplet shear stresses for the three types of sprinkler with three nozzle diameters and two operating pressures. It was found that average droplet shear stresses increased exponentially with the increase of distance from sprinkler. Distribution ranges of average droplet shear stresses along spray direction were 26.94–3313.51, 33.34–2650.80, and 16.15–2485.69 N/m² for D3000, R3000, and KPT sprinklers, respectively.

Droplet shear stress of D3000 was the highest, followed by R3000 and KPT. It was also observed that average droplet shear stresses near sprinkler were very close for different operating pressures and nozzle diameters for any type of low-pressure sprinkler. For instance, the maximum differences of average droplet shear stresses for D3000 were 30.48 and 35.59 N/m² at 1 and 2 m from sprinkler, respectively. Corresponding values for R3000 were 124.04 and 112.32 N/m², respectively, whereas for KPT, the values were 41.05 and 58.10 N/m², respectively. Although average droplet shear stress differences of R3000 at these two distances were larger than those of other two sprinklers, the differences were only 7.66% and 6.93% of average value of the maximum shear stresses (1619.87 N/m²) under different working conditions from the entire jet trajectory.

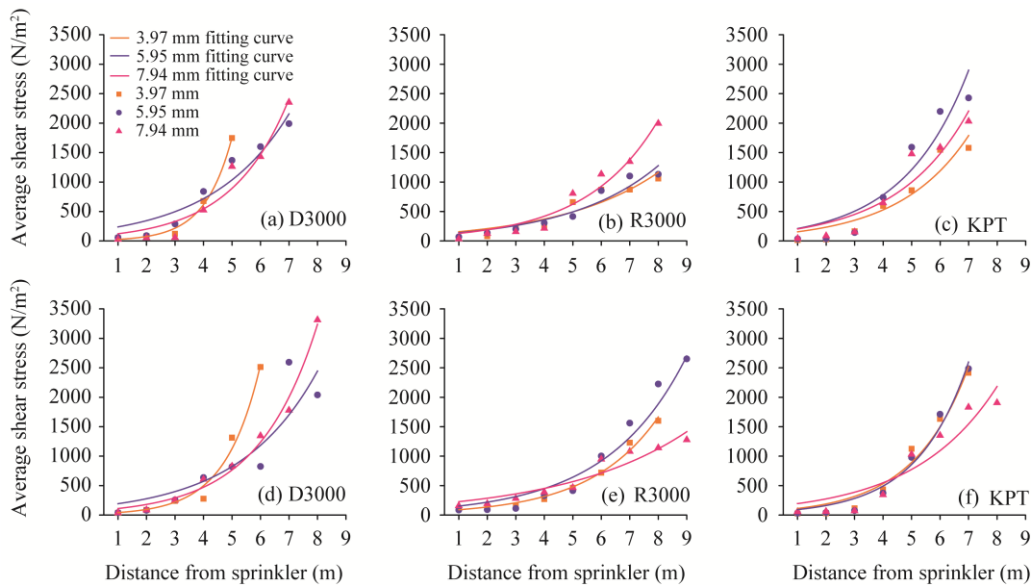


Fig. 13 Distributions of average droplet shear stresses along spray direction for the three types of sprinkler with three nozzle diameters and two operating pressures. (a–c), 103 kPa; (d–f), 138 kPa.

Another unexpected result was that the greater difference in average droplet shear stress was associated with the larger distance from sprinkler. The maximum difference of average droplet shear stresses at the end of the jet reached the values of 1566.81, 1589.64, and 905.77 N/m² for D3000, R3000, and KPT, respectively. The main reason for such a significant difference was attributed to the fact that the higher operating pressure could result in a greater droplet shear stress at the end of the jet. Furthermore, when operating pressure was kept constant, shear stress increased gradually with the increase of nozzle diameter. Therefore, droplet shear stress under larger operating pressure and nozzle diameter was subtracted from corresponding value under smaller ones, and an extraordinarily appreciable difference was obtained.

Table 8 showed exponential regression correlations between average droplet shear stresses and distances from sprinkler for the three types of sprinkler with three nozzle diameters and two operating pressures. Obviously, fitting accuracy of these correlations (R^2 values of more than 0.860) under different treatments of these sprinklers was good, indicating a close relationship between droplet shear stress and distance. This study reintegrated the data of average droplet shear stress and distance from sprinkler under different working conditions, and the universal correlation (Eq. 7) suitable for low-pressure sprinklers was successfully obtained. From the comparative analysis of simulated average shear stresses and measured values (Fig. 14), MAE and RMSE values were 370.246 and 718.291 N/m², respectively. Thus, the accuracy of the universal correlation was not good, although its goodness of fit was satisfactory.

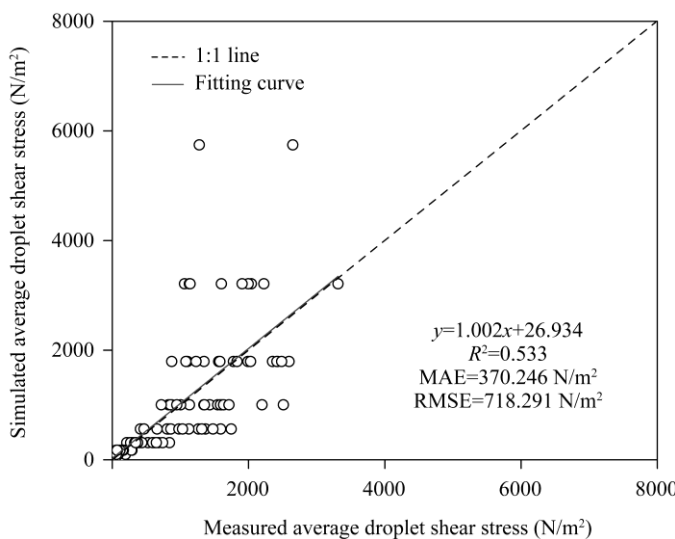
$$\overline{S_s} = 30.562 e^{0.582l}, R^2 = 0.848, \quad (7)$$

where $\overline{S_s}$ is the average droplet shear stress (N/m²); and l is the distance from sprinkler (m).

Table 8 Regression analysis between average droplet shear stress and distance from sprinkler under the three types of sprinkler with three nozzle diameters and two operating pressures

Sprinkler type	Operating pressure (kPa)	Nozzle diameter (mm)	Fitting coefficient		R^2
			μ	φ	
D3000	103	3.97	9.449	1.045	0.992
		5.95	165.550	0.367	0.899
		7.94	74.574	0.497	0.938
	138	3.97	18.912	0.818	0.978
		5.95	34.461	0.576	0.919
		7.94	69.058	0.481	0.986
R3000	103	3.97	118.394	0.286	0.869
		5.95	101.120	0.317	0.911
		7.94	85.905	0.397	0.951
	138	3.97	60.009	0.415	0.986
		5.95	107.010	0.359	0.938
		7.94	181.426	0.228	0.898
KPT	103	3.97	103.809	0.407	0.879
		5.95	136.601	0.436	0.906
		7.94	137.424	0.397	0.872
	138	3.97	67.035	0.518	0.962
		5.95	53.602	0.554	0.968
		7.94	137.830	0.345	0.871

Note: μ and φ are the fitting coefficients of the equation $\bar{S}_s = \mu e^{\varphi l}$.

**Fig. 14** Comparison between simulated and measured average droplet shear stresses obtained by using Equation 7

3.6 Effects of various factors on droplet impact angle, velocity, and shear stress

MANOVA results for the effects of sprinkler type, operating pressure, nozzle diameter, and distance from sprinkler on three parameters of droplet were shown in Table 9. According to the results, sprinkler type and distance from sprinkler exhibited highly significant effects ($P < 0.01$) on droplet impact angle and velocity. Therefore, droplet shear stress was also significantly influenced ($P < 0.05$) by these two factors. Furthermore, results clearly showed that effect of operating pressure on droplet impact angle and velocity achieved a significant level ($P < 0.05$), but it failed to significantly influence ($P > 0.05$) droplet shear stress. These results demonstrated that both

sprinkler type and distance from sprinkler were crucial for the distribution of droplet shear stress. In contrast, the impacts of other two factors (operating pressure and nozzle diameter) were not as significant as expected, although previous analysis reported that they showed certain impacts. Therefore, in the design of low-pressure irrigation systems, appropriate type of sprinkler should be determined. Meanwhile, sprinkler spacing should be carefully selected because it was found to be related to the overlap of droplet shear stress at different distances from sprinkler, and helped in minimizing the risk of soil erosion.

Table 9 Analysis of variance for effects of four influencing factors on three parameters of droplet

Parameter of droplet	Influence factor	Sum of square of deviation	Degrees of freedom	Mean square deviation	F value	P value
Droplet impact angle	Sprinkler type	266.922	2	133.461	31.409	0.000**
	Operating pressure	36.262	1	36.262	8.534	0.004**
	Nozzle diameter	12.930	2	6.465	1.522	0.223
	Distance from sprinkler	6881.943	8	860.243	202.453	0.000**
Droplet velocity	Sprinkler type	2.821	2	1.411	10.040	0.000**
	Operating pressure	0.740	1	0.740	5.266	0.023*
	Nozzle diameter	0.402	2	0.201	1.430	0.243
	Distance from sprinkler	38.601	8	4.825	34.340	0.000**
Droplet shear stress	Sprinkler type	4,421,401.309	2	2,210,700.654	20.833	0.000**
	Operating pressure	18,777.088	1	18,777.088	0.177	0.675
	Nozzle diameter	138,761.362	2	69,380.681	0.654	0.522
	Distance from sprinkler	64,615,904.728	8	8,076,988.091	76.116	0.000**

Note: *, significant difference at $P<0.05$ level; **, significant difference at $P<0.01$ level.

4 Discussion

4.1 Distribution characteristics of droplet impact angle and shear stress

This study systematically analyzed the distributions of droplet impact angle and shear stress of low-pressure sprinklers along the spray direction using 2DVD instrument. It was observed that radial distribution trends of droplet impact angle and shear stress for different low-pressure sprinklers generally remained consistent under various nozzle diameters and operating pressures. That is, larger impact angle and smaller shear stress were observed for the droplets near sprinkler (Chang and Hills, 1993a; Hui et al., 2021a). The reason for this performance might be attributed to the presence of many small-sized droplets that were not far from sprinkler. For the distances of 1, 2, and 3 m from sprinkler, the relative frequencies of droplet diameters within 0–1 mm were as high as 96.1% on average (Hui et al., 2022b). Smaller droplet shows a larger specific surface area (surface area per unit volume), which causes a higher air frictional resistance ratio, thereby making the horizontal velocity of droplet to reduce quickly and approach zero (Chang and Hills, 1993a). Accordingly, horizontal distance traveled by small droplet is short, and its impact angle is almost perpendicular to horizontal plane, resulting in a small shear stress (Hui et al., 2021a). With the increase in distance from sprinkler, droplet impact angle and shear stress gradually decreased and increased, respectively, reaching the minimum and the maximum values at the end of the jet. Hui et al. (2021a) obtained the similar results for radial distribution of droplet impact angle and shear stress using a ball-driven sprinkler. The above-mentioned results revealed that the end of the jet was always prone to surface runoff, which was consistent with the results of the maximum soil erosion position obtained from the perspective of specific power (Silva, 2006; Yan et al., 2011; King and Bjorneberg, 2011; Hui et al., 2022b). Accordingly, the specific power and droplet shear stress showed a certain similarity in predicting soil erosion of sprinkler irrigation system. Nonetheless, there were significant differences between them in terms of the formation

mechanism, because the shear stress considered the direction of a droplet impacting the ground, while the specific power incorporated the factor of water application rate (Chang and Hills, 1993b; Ge et al., 2018). Therefore, both droplet characteristical parameters exhibited their advantages in evaluating the soil erosion of sprinkler irrigation system. However, it was still uncertain which parameter was better, thus requiring further studies.

4.2 Effect of various factors on the distribution of droplet shear stress

Even though the distributions of droplet shear stress under different treatments in radial direction were generally the same, some differences were observed. Overall, the larger the operating pressure or nozzle diameter, the greater the shear stress. It was worth noticing that the larger operating pressure and nozzle diameter could lead to a bigger radius of throw (Carrión et al., 2001; Ge et al., 2020). Therefore, the above-mentioned difference in droplet shear stress could also be partly attributed to the difference in the radius of throw. However, these differences were non-significant ($P>0.05$) according to MANOVA. These findings were in good agreement with the results reported by Hui et al. (2021a), who found that although the nozzle diameter had a certain effect on the maximum shear stress, the overall effect was insignificant. In addition to droplet shear stress, kinetic energy and specific power of low-pressure sprinkler were also found to be insignificantly affected ($P>0.05$) by operating pressure and nozzle diameter (Hui et al., 2022b), but this result was not supported by Bautista-Capetillo et al. (2012) on a VYR35 sprinkler and Osman et al. (2015) on a double nozzle impact sprinkler. One possible explanation is that their studies were conducted based on medium- and high-pressure sprinklers such as impact sprinklers. These sprinklers are fundamentally different from the spraying methods of low-pressure sprinklers. On the other hand, they selected a larger distribution range of operating pressures and nozzle diameters in the experiments, which could easily lead to significant differences in droplet characteristics. In this study, highly significant ($P<0.01$) differences in the distributions of droplet shear stresses were found among different types of low-pressure sprinklers, which were due to their different nozzle structures and spraying characteristics, as previously reported by Faci et al. (2001) on the distributions of droplet diameters for various types of low-pressure sprinkler. Among them, the average shear stress range of D3000 attained the largest value, followed by R3000 and KPT. It was suggested that FSPS was prone to generating significant droplet shear stress. Therefore, direct spraying on the bare ground should be avoided in the field irrigation to prevent severe soil erosion. In contrast, it was recommended to promote the application of OSPS in irrigation engineering due to its smallest shear stress among the three types of low-pressure sprinkler, which was in line with the results reported by Hui et al. (2022b) for the optimization of center pivot irrigation system from the perspective of droplet kinetic energy.

4.3 Limitation and suggestion

This research can provide a new possibility for the accurate prediction and prevention of soil erosion in sprinkler irrigation systems, and it can also show an important reference value for the transformation of low-pressure sprinkler irrigation systems. However, there are some limitations. In this study, the correlations among various indicators such as droplet impact angle, velocity, shear stress, and distance from the sprinkler were developed. We observed weak correlations between droplet impact angle and velocity (MAE and RMSE of 7.876° and 9.627° , respectively) and between average droplet shear stress and distance from the sprinkler (MAE and RMSE of 370.246 and 718.291 N/m², respectively). The reason might be that the accuracy of correlations was affected by the data errors due to droplet splashing, although a significant portion of the error was processed by the statistical tests based on the 3σ criterion (Jiang et al., 2021). Therefore, it is critical to further standardize the droplet testing process to minimize experimental error in future studies. Moreover, it should be noted that the universal correlations developed in this study were based on only the three types of low-pressure sprinklers of D3000, R3000, and KPT. Actually, there are many types of low-pressure sprinkler from different manufacturers, which exhibit

differences in the droplet distribution (King and Bjorneberg, 2012b). Therefore, it is necessary to supplement the droplet data of more sprinklers to improve the universalities of the developed correlations. In addition, the droplet distribution test of a single sprinkler in this study was conducted under indoor conditions, while the actual sprinkler irrigation system is usually used in the field. Accordingly, future research should consider the effects of meteorological factors, including wind velocity, direction, temperature, humidity, and solar radiation on the distributions of droplet impact angle and shear stress. More importantly, it is necessary to further compare the effects of specific power and droplet shear stress on the soil infiltration under the same sprinkler irrigation condition to reveal which of these two droplet characteristical parameters has a greater impact on soil erosion. Furthermore, a center pivot irrigation system is composed of multiple sprinklers. The spraying method of multiple sprinklers is more complicated than that of a single sprinkler. Some of the droplets between adjacent sprinklers may collide with each other during the movement (Ge et al., 2015). This phenomenon can lead to unpredictable changes in the diameter, velocity, and shear stress of the droplet. Therefore, it is highly desirable to conduct future research regarding the droplet characteristics and their impacts on crop growth under the center pivot irrigation system with multiple sprinklers.

5 Conclusions

Lower droplet shear stresses under different types of sprinkler, operating pressures, and nozzle diameters generally occurred near the sprinkler. However, with the increase in the distance from the sprinkler, the shear stress continuously increased and reached a peak value at the end of the jet, indicating that the highest risk of soil erosion occurred at the jet end, and the soil erosion in the sprinkler irrigation system could not only be simply attributed to the droplet kinetic energy, but also required consideration in combination with the shear stress. Moreover, sprinkler type and distance from sprinkler were found to play key roles in the radial distribution of droplet shear stress. Although the operating pressure showed a significant effect on the distribution of shear stress, its overall effect was non-significant. Therefore, when designing low-pressure irrigation systems, compared with adjusting the nozzle diameter and operating pressure, it was more important to reasonably select the sprinkler type and sprinkler spacing to reduce soil erosion. In this study, we found that D3000 exhibited the largest radial average shear stress ranges among the three types of low-pressure sprinkler, followed by R3000 and KPT. In order to minimize the soil erosion by reducing droplet shear stress, KPT sprinkler was undoubtedly more suitable than D3000 and R3000 sprinklers for the promotion in center pivot irrigation systems.

Acknowledgements

The study was funded by the National Natural Science Foundation of China (51939005), the Key Research and Development Program of Hebei Province, China (21327002D), the Hebei Forage Industry Innovation Team of Modern Agro-industry Technology Research System of China (HBCT2018160202), the Regional Collaborative Innovation Project of Xinjiang Uygur Autonomous Region of China (2021E02056), and the China Agriculture Research System of Ministry of Finance and Ministry of Agriculture and Rural Affairs (CARS-34).

References

- Al-Kayssi A W, Mustafa S H. 2016. Modeling gypsumiferous soil infiltration rate under different sprinkler application rates and successive irrigation events. *Agricultural Water Management*, 163: 66–74.
- Baiamonte G, Provenzano G, Iovino M, et al. 2021. Hydraulic design of the center-pivot irrigation system for gradually decreasing sprinkler spacing. *Journal of Irrigation and Drainage Engineering*, 147(7): 04021027, doi: 10.1061/(ASCE)IR.1943-4774.0001568.
- Bautista-Capetillo C, Zavala M, Playán E. 2012. Kinetic energy in sprinkler irrigation: different sources of drop diameter and velocity. *Irrigation Science*, 30(1): 29–41.
- Carrión P, Tarjuelo J, Montero J. 2001. SIRIAS: a simulation model for sprinkler irrigation. *Irrigation Science*, 20(2): 73–84.

chinaXiv:202211.00145v1

- Chang W J, Hills D J. 1993a. Sprinkler droplet effects on infiltration. II: laboratory study. *Journal of Irrigation and Drainage Engineering*, 119(1): 157–169.
- Chang W J, Hills D J. 1993b. Sprinkler droplet effects on infiltration. I: impact simulation. *Journal of Irrigation and Drainage Engineering*, 119(1): 142–156.
- Chen R, Li H, Wang J, et al. 2020. Effects of pressure and nozzle size on the spray characteristics of low-pressure rotating sprinklers. *Water*, 12(10): 2904, doi: 10.3390/w12102904.
- De Jong S M, Addink E A, Van Beek L P H, et al. 2011. Physical characterization, spectral response and remotely sensed mapping of Mediterranean soil surface crusts. *CATENA*, 86(1): 24–35.
- Etikala B, Adimalla N, Madhav S, et al. 2021. Salinity problems in groundwater and management strategies in arid and semi-arid regions. *Groundwater Geochemistry: Pollution and Remediation Methods*, 42–56.
- Faci J M, Salvador R, Playán E, et al. 2001. Comparison of fixed and rotating spray plate sprinklers. *Journal of Irrigation and Drainage Engineering*, 127(4): 224–233.
- Ferreira A G, Larock B E, Singer M J. 1985. Computer simulation of water drop impact in a 9.6-mm deep pool. *Soil Science Society of America Journal*, 49(6): 1502–1507.
- Ge M, Wu P, Zhu D, et al. 2015. Effect of jets interaction on spray characteristics between adjacent sprinklers. *Transactions of the Chinese Society of Agricultural Engineering (Transactions of the CSAE)*, 31(9): 100–106. (in Chinese)
- Ge M, Wu P, Zhu D, et al. 2018. Analysis of kinetic energy distribution of big gun sprinkler applied to continuous moving horse-drawn traveler. *Agricultural Water Management*, 201: 118–132.
- Ge M, Wu P, Zhu D, et al. 2020. Comparisons of spray characteristics between vertical impact and turbine drive sprinklers—A case study of the 50PYC and HY50 big gun-type sprinklers. *Agricultural Water Management*, 228: 105847, doi: 10.1016/j.agwat.2017.12.009.
- Ghadiri H, Payne D. 1986. The risk of leaving the soil surface unprotected against falling rain. *Soil & Tillage Research*, 8: 119–130.
- Ghadiri H, Payne D. 2010. The formation and characteristics of splash following raindrop impact on soil. *European Journal of Soil Science*, 39(4): 563–575.
- Huang C, Bradford J M, Cushman J H. 1982. A numerical study of raindrop impact phenomena: the rigid case1. *Soil Science Society of America Journal*, 46(1): 14–19.
- Huang G, Bringi V N, Cifelli R, et al. 2010. A methodology to derive radar reflectivity-liquid equivalent snow rate relations using C-band radar and a 2D video disdrometer. *Journal of Atmospheric & Oceanic Technology*, 27(4): 637–651.
- Hui X, Lin X, Zhao Y, et al. 2022a. Assessing water distribution characteristics of a variable-rate irrigation system. *Agricultural Water Management*, 260: 107276, doi: 10.1016/j.agwat.2021.107276.
- Hui X, Zheng Y, Meng F, et al. 2022b. Comprehensively evaluating and modelling droplet diameters and kinetic energies of low-pressure sprinklers. *Irrigation and Drainage*, 71(4): 829–854.
- Hui X, Zheng Y, Yan H. 2021b. Water distributions of low-pressure sprinklers as affected by the maize canopy under a centre pivot irrigation system. *Agricultural Water Management*, 245: 106646, doi: 10.1016/j.agwat.2020.106646.
- Jiang Y, Liu J, Li H, et al. 2021. Droplet distribution characteristics of impact sprinklers with circular and noncircular nozzles: Effect of nozzle aspect ratios and equivalent diameters. *Biosystems Engineering*, 212: 200–214.
- King B A, Bjorneberg D L. 2011. Evaluation of potential runoff and erosion of four center pivot irrigation sprinklers. *Applied Engineering in Agriculture*, 27(1): 75–85.
- King B A, Bjorneberg D L. 2012a. Transient soil surface sealing and infiltration model for bare soil under droplet impact. *Transactions of the ASABE*, 55(3): 937–945.
- King B A, Bjorneberg D L. 2012b. Droplet kinetic energy of moving spray-plate center-pivot irrigation sprinklers. *Transactions of the ASABE*, 55(2): 505–512.
- Kruger A, Krajewski W F. 2002. Two-dimensional video disdrometer: A description. *Journal of Atmospheric & Oceanic Technology*, 19(5): 602–617.
- Lu J, Zheng F, Li G, et al. 2016. The effects of raindrop impact and runoff detachment on hillslope soil erosion and soil aggregate loss in the Mollisol region of Northeast China. *Soil and Tillage Research*, 161: 79–85.
- Manke E B, Norenberg B G, Faria L C, et al. 2019. Wind drift and evaporation losses of a mechanical lateral-move irrigation system: oscillating plate versus fixed spray plate sprinklers. *Agricultural Water Management*, 225: 105759, doi:

10.1016/j.agwat.2019.105759.

- Osman M, Hassan S B, Yusof K. 2015. Effect of combination factors of operating pressure, nozzle diameter and riser height on sprinkler irrigation uniformity. *Applied Mechanics & Materials*, 695: 380–383.
- Robles O, Playán E, Cavero J, et al. 2017. Assessing low-pressure solid-set sprinkler irrigation in maize. *Agricultural Water Management*, 191: 37–49.
- Robles O, Zapata N, Burguete J, et al. 2019. Characterization and simulation of a low-pressure rotator spray plate sprinkler used in center pivot irrigation systems. *Water*, 11(8): 1684, doi: 10.3390/w11081684.
- Sayyadi H, Nazemi A H, Sadraddini A A, et al. 2014. Characterising droplets and precipitation profiles of a fixed spray-plate sprinkler. *Biosystems Engineering*, 119: 13–24.
- Silva L L. 2006. The effect of spray head sprinklers with different deflector plates on irrigation uniformity, runoff and sediment yield in a Mediterranean soil. *Agricultural Water Management*, 85(3): 243–252.
- Silva L L. 2007. Fitting infiltration equations to centre-pivot irrigation data in a Mediterranean soil. *Agricultural Water Management*, 94(1–3): 83–92.
- Stambouli T, Martínez-Cob A, Faci J M, et al. 2013. Sprinkler evaporation losses in alfalfa during solid-set sprinkler irrigation in semiarid areas. *Irrigation science*, 31(5): 1075–1089.
- Vaezi A R, Ahmadi M, Cerdà A. 2017. Contribution of raindrop impact to the change of soil physical properties and water erosion under semi-arid rainfalls. *Science of the Total Environment*, 583: 382–392.
- Yan H, Jin H, Qian Y. 2010. Characterizing center pivot irrigation with fixed spray plate sprinklers. *Science China Technological Sciences*, 53(5): 1398–1405.
- Yan H, Bai G, He J, et al. 2011. Influence of droplet kinetic energy flux density from fixed spray-plate sprinklers on soil infiltration, runoff and sediment yield. *Biosystems Engineering*, 110(2): 213–221.
- Yan H, Hui X, Li M, et al. 2020. Development in sprinkler irrigation technology in China. *Irrigation and Drainage*, 69(52): 78–87.